Kapal: Jurnal Ilmu Pengetahuan dan Teknologi Kelautan
(Kapal: Journal of Marine Science and Technology)
journal homepage : http://ejournal.undip.ac.id/index.php/kapal
2301-9069 (e)
1829-8370 (p)

# CFD Analysis Into the Resistance of Trimaran with Longitudinal Side hull Adjustments

Richard Benny Luhulima1)*), Sutiyo2) , I Ketut Aria Pria Utama3)

1) Department of Naval Architecture, Faculty of Engineering, Pattimura University, Ambon 97233, Indonesia
2) Department of Naval Architecture, Faculty of Engineering and Marine Science, Hang Tuah University, Surabaya 60111, Indonesia
3) Department of Naval Architecture, Faculty of Marine Technology, Sepuluh Nopember Institute of Technology, Surabaya 60111, Indonesia
*) Corresponding Author: richardluhulima26@gmail.com

**Article Info**

**Keywords:**
Trimaran;
CFD;
Resistance; Interference;
R/L Variation

**Article history:**
Received: 28/08/2021
Last revised: 24/10/2021
Accepted: 25/10/2021
Available online: 25/10/2021
Published: 31/10/2021

**DOI:**
https://doi.org/10.14710/kapal.v18i3.41010

**Abstract**

There has recently been a surge in demand for multi-hull vessels for military and commercial purposes. The need for multi-hull ships increase from the necessity to balance speed and cargo requirements. Among others, the trimaran is one such hull type. The current study performs a CFD resistance analysis for trimaran as a parameter range of feasible hull forms based on the NPL systematic series. The resistance of trimaran hull shapes are calculated using CFXTM, a commercial CFD code that belongs to ANSYS. The trimaran model was tested at one fixed transverse separation (S/L=0.2) together with 3 longitudinal separations, R/L=0, 0.25, and 0.5, at different Froude numbers (based on length) from 0.2 to 0.6. Testing on the individual hull is also carried out to quantify the effect of resistance interference on the trimaran configuration. The CFD simulation results indicate that the trimaran model with side hulls parallel to the stern (R/L=0) has the least resistance. The interference effect of resistance on Trimaran with R/L=0, 0.25, 0.5 are 2.8%, 4.6%, 6.8% as opposed to non-interference trimaran model, respectively. These findings provide an approach for appropriately selecting the trimaran model with longitudinal side hull configurations.



## 1. Introduction

Indonesia has more than 5.9 million square kilometers of public waters, making it the second-largest in Asia behind China [1]. The marine sector is particularly important to Indonesia since it covers a wide range of factors, including economics, law, defense, security, the environment, and socio-cultural influences. The state of the distinct islands has the result that sea transportation facilities are required, which are critical components of economic development on a national and worldwide scale. The port serves as an essential infrastructure in the growth of the area economy, particularly in the distribution of development [2].

Maritime shipping is important considering Indonesia is a large archipelago that requires an infrastructure of ports in order to be connected. Container ships, ferries, passenger ships, sailing ships, and motorized vessels are examples of widely used boats. Even though the local people in Indonesia prefer the older ship designs, the wooden pinisi is still utilized to transport people and cargo from island to island. Jakarta's Sunda Kelapa is the best-known traditional maritime port, while Makassar's Paotere harbor is the other major traditional port.

Many islands are served by large rivers, which offer an essential transit route because of poor roadways. The only method to get interior on Kalimantan is via longboat on the rivers. Trimaran boats are gaining popularity owing to their benefits and uses [3]. For ship stability, the trimaran features side hulls. The trimaran's three hulls make it unsinkable. Even in the most severe weather, the final risk of capsizing is reduced. The main hull and side hulls may be easily changed to reduce resistance [4]. Consequently, as trimaran resistance decreases, so does fuel consumption compared to a comparable monohull.

Numerous studies have been conducted over the past decades to determine the benefits of the trimaran idea. Whenever the trimaran literature is evaluated in general, it is apparent that the most critical parameter for resistance optimization is the design of the outriggers due to the flow interference effect between the center-hull and outriggers [5]. Their optimal location will result in an interaction between the wave trains generated by the center-hull and the outriggers, which will ideally counterbalance each other at the main speed(s) of interest [6].

Gray conducted preliminary trimaran studies [7]. The resistance properties of a trimaran hull shape were studied in this research to check the theoretical prediction compared to the test findings. Heidari et al. used the CFD technique to evaluate

the hydrodynamic performance of trimaran hull forms with tiny extinguishers to find optimal wave resistance outrigger locations [8]. The wave interactions between the center hull and the pushing devices were also examined to estimate overall wave resistance.

The CFD program was used to examine how a trimaran hull's resistance might be predicted [9]. The effects of mesh structure and turbulence models on the resistance predictions were examined using several mesh sizes and turbulence models. To compare CFD findings with experimental data, results were found using low to medium Froude Number, and the analyses were compared with experimental data. Son conducted Computational Fluid Dynamics (CFD) calculations on a variety of trimaran hull shapes [10]. The trimaran was designed using a formula with a center hull design based on the NPL's round bilge hull and scaled side hulls. The location of the side hull has a profound effect on ship resistance, Poundra et al. pointed out because it has a strong influence on both the longitudinal and transverse dynamics [11]. Trimarans also experience this interference phenomenon to a greater degree. Flow field interaction between trimaran ships' hulls is shown by Sun et al. [12] using numerical calculations and PIV experiments to show the flow field between the main hull and the side hull can be recorded with a high resolution in both microscopic and macroscopic structure. Residual resistance levels may be reduced by using the right trimaran arrangements [13]. However, the previous study did not include the effects of side hull placement longitudinally, from stern to bow.

In this study, the main objective is to analyze the resistance of trimaran vessels by utilizing the CFD method based on RANS (Reynolds-Averaged Navier-Stokes). The analysis was carried out on the trimaran model S/L=0.2 with variations of R/L on Froude numbers 0.2 to 0.6. A brief introduction of the CFD solver is presented, followed by a description of the numerical setup consisting of mesh generation and boundary conditions. The interference effect is calculated to determine its effect on the model resistance. Finally, the optimum trimaran configuration will be achieved.

## 2. Methods

### 2.1. Modeling

The research was conducted on a trimaran ship with a configuration of S/L=0.2 (Separation, S=0.25 m), as shown in Figure 1. Furthermore, the trimaran model was analyzed for CFD simulation at Fr=0.2 – 0.6. The geometry parameters of the trimaran hull are presented in Table 1.

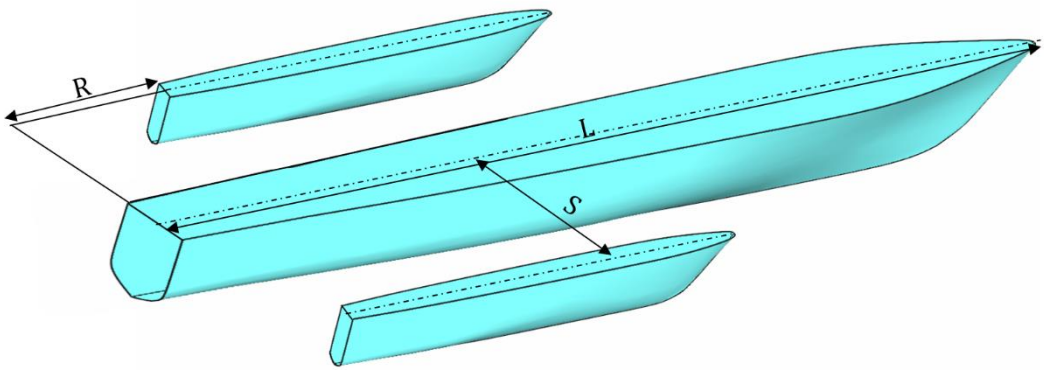


Figure 1. Trimaran Model.

Table 1. Parameter Dimension of Model

| Parameter | Unit | Main hull | Side hull |
|---|---|---|---|
| $L_{OA}$ | m | 1.252 | 0.621 |
| $L_{WL}$ | m | 1.208 | 0.573 |
| B | m | 0.113 | 0.056 |
| T | m | 0.103 | 0.058 |
| Wetted Surface Area | $m^2$ | 0.256 | 0.041 |
| Displacement | kg | 7.171 | 0.362 |
| Block Coefficient ($C_B$) | | 0.467 | 0.490 |

This study was conducted on trimaran ships with varying longitudinal and parallel side hull placement, as indicated in Figure 2. Variation 1, as illustrated in Figure 2(a), has a side hull parallel to the main hull on the stern. Variation 2 depicts the side hull midship parallel to the main hull midship, as shown in Figure 2(b). In contrast, variation 3 portrays the side hull bow section parallel to the main hull bow section, as depicted in Figure 2(c).

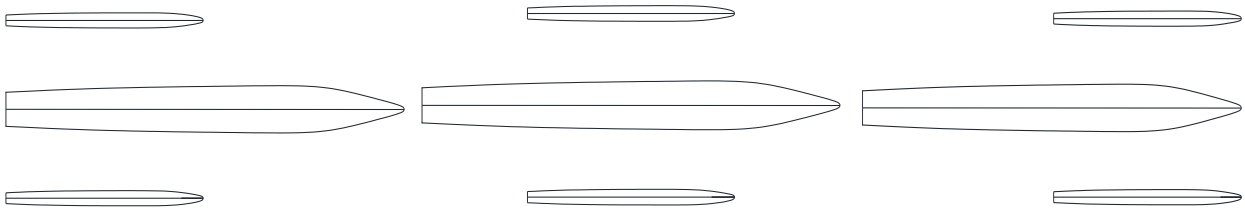

(a) Trimaran A (R/L=0) (b) Trimaran B (R/L=0.25) (c) Trimaran C (R/L=0.5)

Figure 2. Longitudinal Configuration.

## 2.2. Governing Equation

A three-dimensional equation created and utilized in the CFD model is the Reynolds-averaged Navier-Stokes (RANS) technique. Incompressible flow equations created by ANSYS-CFX software are used to address flow issues in ship walls. The averaged continuity and momentum equations are provided for incompressible flows in the following two equations [14]. In Equations (1) and (2), the mass and momentum equations are expressed as follows:

$$\frac{\partial \rho}{\partial t} + \nabla . (\rho U) = 0 \tag{1}$$

$$\frac{\partial (\rho U)}{\partial t} + \nabla . (\rho U \; x \; U) = -\nabla p + \nabla . \tau + S_M \tag{2}$$

Where the stress tensor, τ is related to the strain rate.

Furthermore, Reynolds Averaged Navier-Stokes (RANS) was developed, which is a variation of unstable Navier-Stokes incorporating averaged and fluctuating parameters. Anderson [15] defines the turbulence model based on the RANS equation as a statistical turbulence model produced by the statistical average method used to derive the equations. The average equations of RANS are provided in Equations (3) and (4):

$$\frac{\partial \rho}{\partial t} + \frac{\partial}{\partial x_j}(\rho U_j) = 0 \tag{3}$$

$$\frac{\partial (\rho U)}{\partial t} + \frac{\partial}{\partial x_j}(\rho U_i U_j) = -\frac{\partial p}{\partial x_j} + \frac{\partial}{\partial x_j}(\tau_{ij} - \overline{\rho u_i u_j}) + S_M \tag{4}$$

where τ is the stress tensor molecular consisting of normal and shear stress components

The near-wall performance of the k- ω appealing model may be employed without the possibility of causing inconsistencies to its free stream sensitivity, and it provides highly precise predictions of the start and magnitude of flow separation under undesirable pressure gradients [16]. The SST model has benefited greatly from the strength of the fundamental turbulence model, which is why the development of an accurate and dependable near-wall formulation of the Wilcox model has greatly aided its industrial application of turbulence, heat, and mass transport [17]. This is further supported by Utama et al. [13] comprehensive research of trimaran ships.

## 2.3. Boundary Condition

The most often recommended computational domain for simulating at a velocity intake was placed 2L ahead perpendicular to the front and a pressure outlet of 5L toward the back, also perpendicularly. The transverse and vertical directions were both set in order to counteract the effects of transverse pressure [18]. In order to prevent backflow, Ford and Winroth implemented a pressure exit outflow for the downstream boundary condition [19], as illustrated in Figure 3.

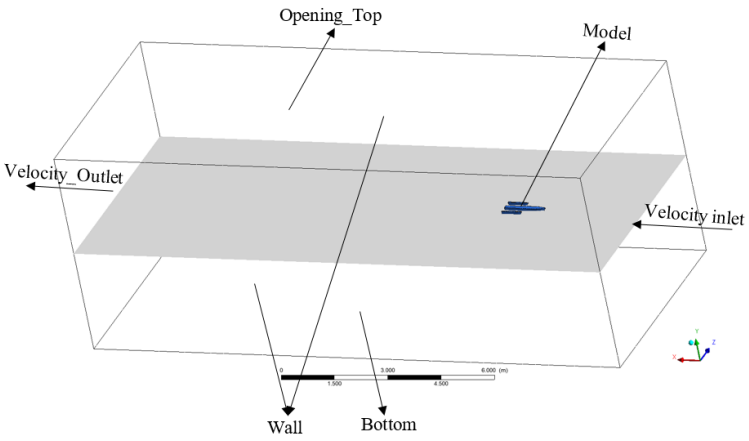


Figure 3. Boundary Conditions.

## 2.4. Grid Independence

The use of an unstructured mesh in any part of grid creation offers several benefits over using a structured mesh. The use of an inflation mesh enables the CFD to correctly complete flow along the model's wall by characterizing the flow separation near the hull of the model [20], as shown in Figure 4.

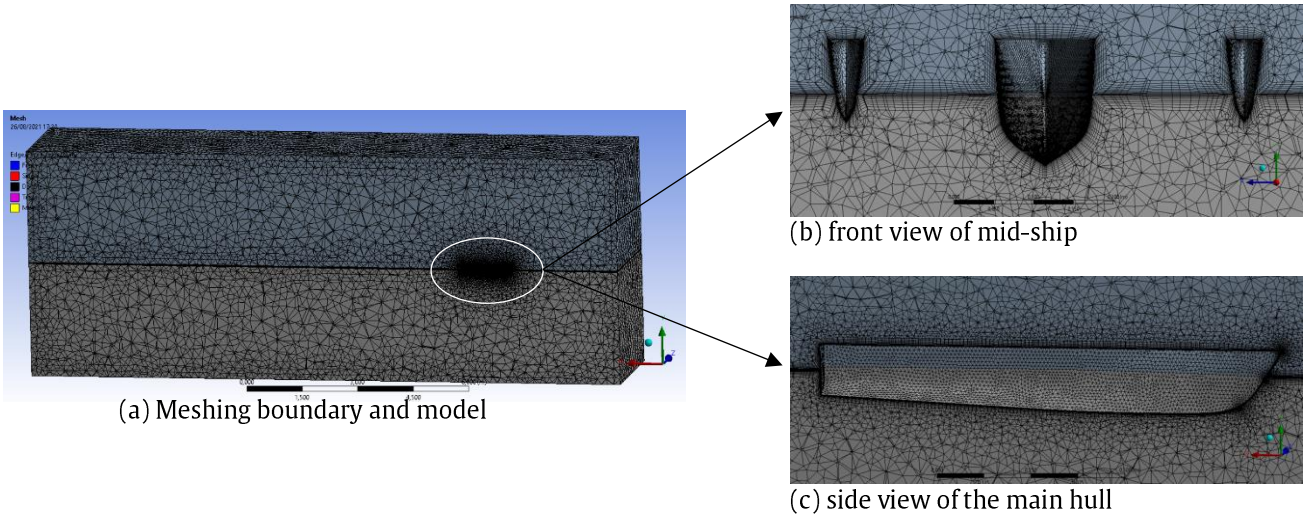

(a) Meshing boundary and model

(b) front view of mid-ship

(c) side view of the main hull

Figure 4. Meshing Trimaran Model with Unstructured mesh and inflation.

Consistency and history records that represent the working period of a variable amplitude deviation comprehensive approach to CFD simulation are critical aspects of the numerical simulation calculation. Convergence and history records are important aspects of numerical simulation calculation. The root-mean-square (RMS) criterion was employed to verify for convergence, with the residual target value (variable value) approaching 10-4 and the results given in Figure 5(a) indicating that the model is converging. A well-posed issue and a closely converging solution are indicated by the presence of monotonic convergence in these residual monitors. Accurate findings are directly correlated to the quantity of cells or grids used in calculations. A project plan in which the number of meshing is determined independently was used in the illustration as shown in Figure 5(b). Simulation grid independence of Trimaran A with Fr = 0.3 was conducted. Results obtained from grid independence tests indicated that with a total resistance coefficient of 0.098 to optimum difference CT of 1.02 percent, where trimaran model simulations on grid number 1,698,532 are the best.

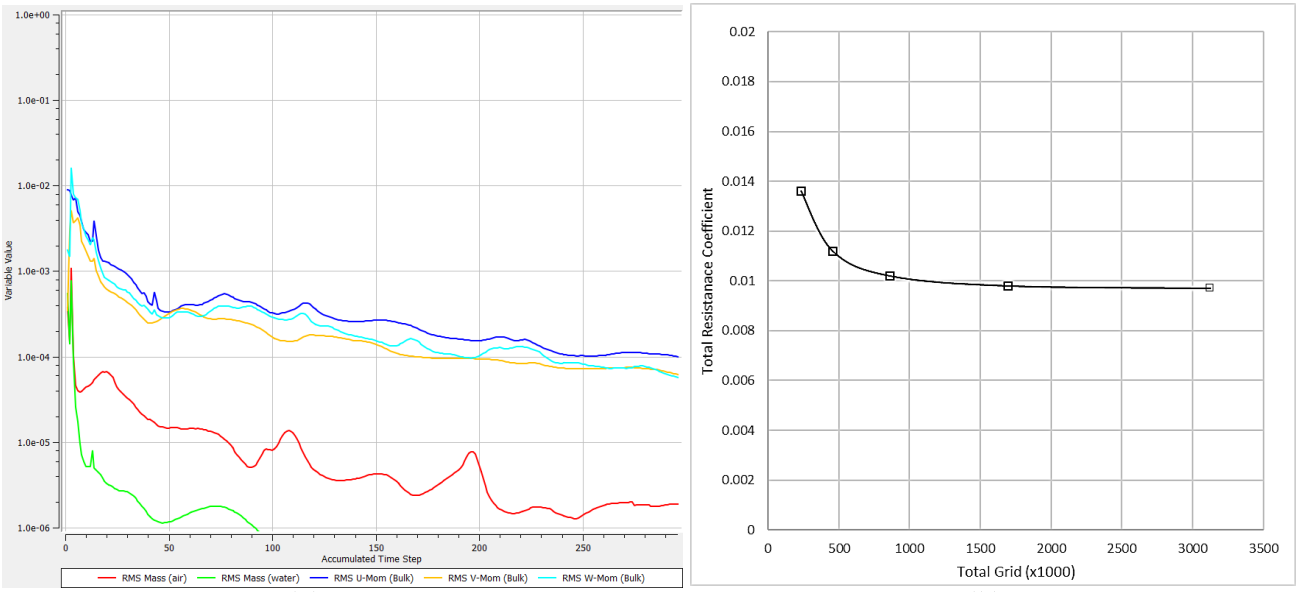


(a) (b)

Figure 5. (a) Convergence; (b) Grid Independence Study.

## 3. Results and Discussion

### 3.1. Trimaran Non-Interference

The Trimaran Non-Interference model has been designed to simulate separately for CFD, with the main hull and side hull simulated of Fr=0.2-0.6, respectively. According to Utama et. al [13], the formula for calculating the non-interference trimaran resistance is as follows:

$$C_{T\_Trimaran\ (NI)} = C_{T_{Mainhull}} + 2C_{T\_SIdehull} \quad (5)$$

Where $C_{T\_Trimaran\ (NI)}$ is the total resistance of Trimaran with no interference, $C_{T_{Mainhull}}$ is the total resistance of the main hull, and $C_{T\_SIdehull}$ is the total resistance of the Side hull.

The results of the non-interference Trimaran and each hull are depicted in Figure 6. The calculation of the resistance on the main hull tends to increase, whereas the calculation on the side hull tends to decrease. This has a positive impact on the $C_T$ of trimaran non-interference ($C_{T\,trimaran}^{NI}$) value.

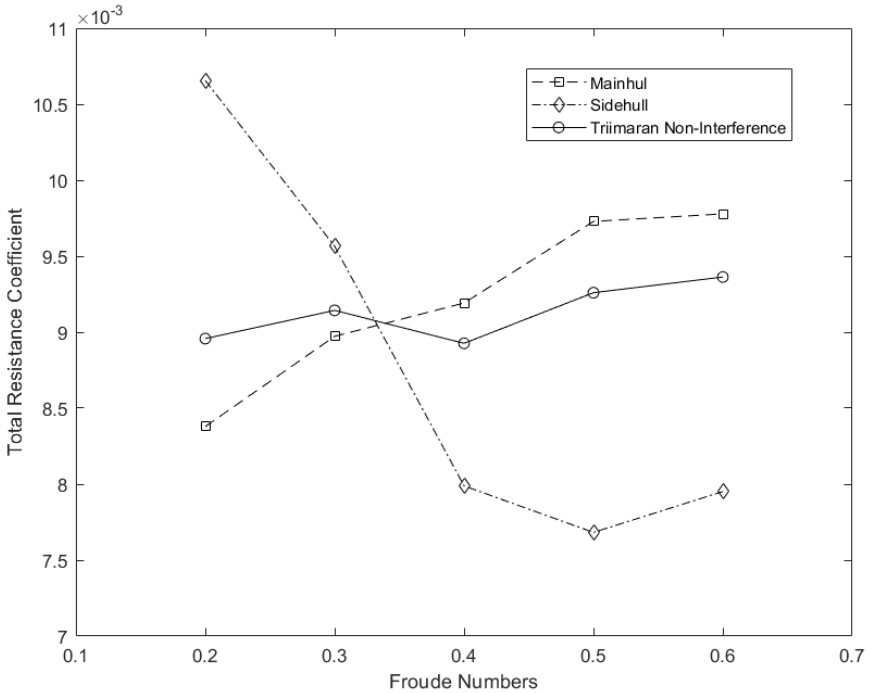


Figure 6. Total Resistance Coefficient of the Main hull and Side hull.

The significant difference in the resistance trend occurs in the main hull and side hull as shown in Figure 6. This is due to the significant difference in the draft, which also affects the WSA of side hulls to be much smaller than the WSA of the main hull. This causes the wave phenomenon created by the side hull to be much smaller when compared to the main hull, especially at Fr>0.3.

CFD simulation at low speed with Fr <0.3 side hull has a negative effect on $C_{T\,trimaran}^{NI}$ whereas the main hull has a positive effect with $C_{T\,trimaran}^{NI}$ reduction. While at Fr> 0.3, the side hull has a positive effect on reducing $C_{T\,trimaran}^{NI}$ and the main hull has a negative effect with a significant increase in $C_{T\,trimaran}^{NI}$. The flow that hits the main hull is quite large which results in a significant change in the flow pattern around the ship as shown in Figures 7 and 8.

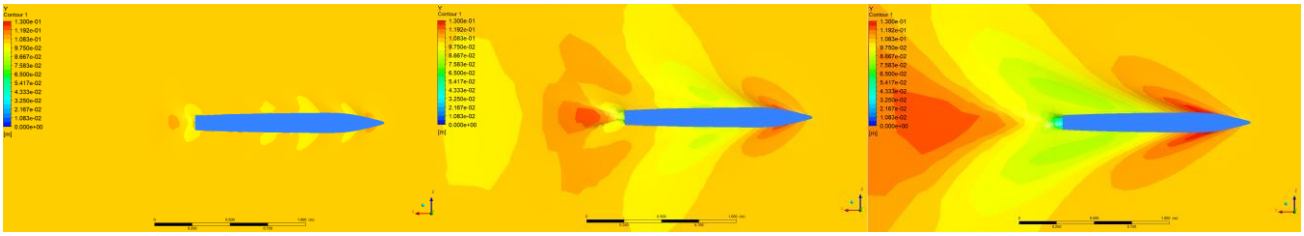

(a) Fr = 0.2 (b) Fr = 0.4 (c) Fr = 0.6

Figure 7. Velocity Distribution of Main Hull

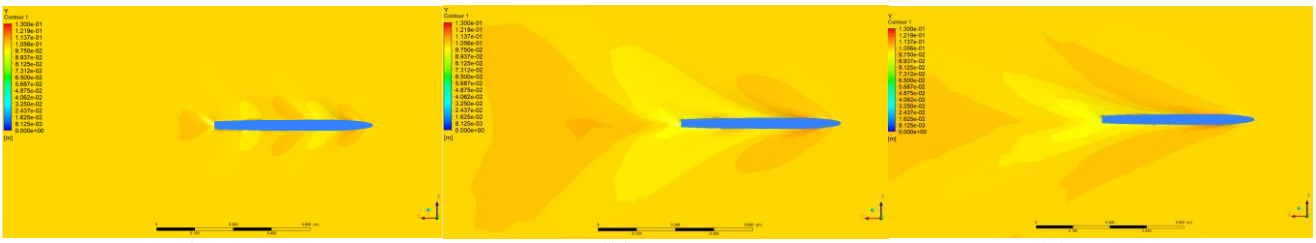

(a) Fr = 0.2 (b) Fr = 0.4 (c) Fr = 0.6

Figure 8. Velocity Distribution of Side Hull.

### 3.2. Trimaran With-Interference

The resistance of the trimaran ship was calculated using the following formula [13] :

$$C_{T\_Trimaran} = C_{T_{Mainhull}} + 2C_{T\_SIdehull} + \Delta C_{T\_Trimaran} \quad (6)$$

Where $C_{T\_Trimaran}$ is the total resistance of Trimaran, $C_{T_{Mainhull}}$ is the total resistance of the main hull, and $C_{T\_Sidehull}$ is the total resistance of Side hull, $\Delta C_{T\_Trimaran}$ is an interference of trimaran total resistance. Thus, interference is defined as the difference between the total resistance of non-interference and interference of the multi-hull ship configuration. Despite the complexity of multi-hull total resistance components, interference effects may be observed experimentally. An IF measures the degree of interaction between the hulls of a multihull [13]. IF is formulated in Equation (7), as follows:

$$IF = \frac{\Delta C_{T\,trimaran}\left[C_{T\,trimaran} - C_{T\,trimaran\,(NI)}\right]}{C_{T\,trimaran}\,(NI)} \quad (7)$$

Where: IF is Interference Factor, $\Delta C_{T\,trimaran}$ is a difference in resistance coefficient between multihull ship non-interference and with interference $(C_{T\,timaran} - C_{T\,trimaran\,(NI)})$, $C_{T\,trimaran\,(NI)}$is the total resistance coefficient of multihull non-interference.

The simulation results of different Trimaran variants' total resistance coefficients are presented in Figure 9. The Trimaran model's $C_T$ fluctuation trend is consistent across variants, with $C_T$ increasing at Fr=0.3, then decreasing at Fr=0.4, then increasing again at Fr above 0.5. The evidence lies in the above-mentioned tests, as well as the examination by Utama et al. [13].

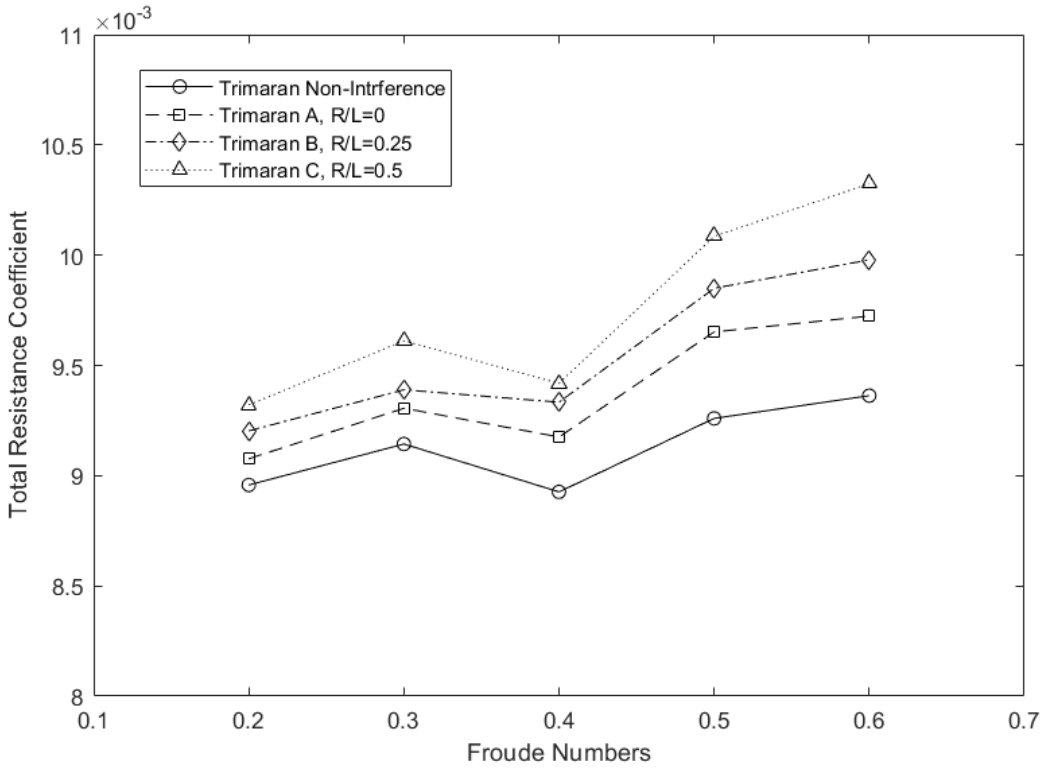


Figure 9. Total Resistance Coefficient of Trimaran.

The longitudinal side hull positioning has a relatively significant difference in $C_T$ values. Non-interference Trimaran has a smaller $C_T$ compared to other variations with an average difference of 2.8% compared to Trimaran A, 4.6% against Trimaran B, and 6.8% alongside Trimaran C. This difference is caused by the interference effect between the main hull and side hull trimaran models.

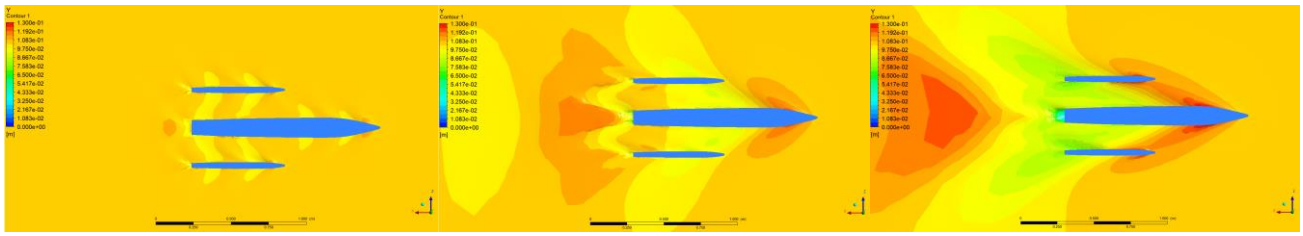

(a) Fr = 0.2 (b) Fr = 0.4 (c) Fr = 0.6

Figure 10. Velocity Distribution of Trimaran A.

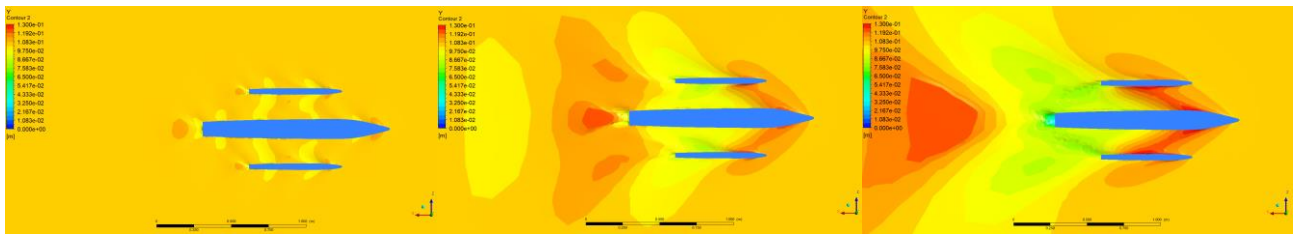

(a) Fr = 0.2 (b) Fr = 0.4 (c) Fr = 0.6

Figure 11. Velocity Distribution of Trimaran B.

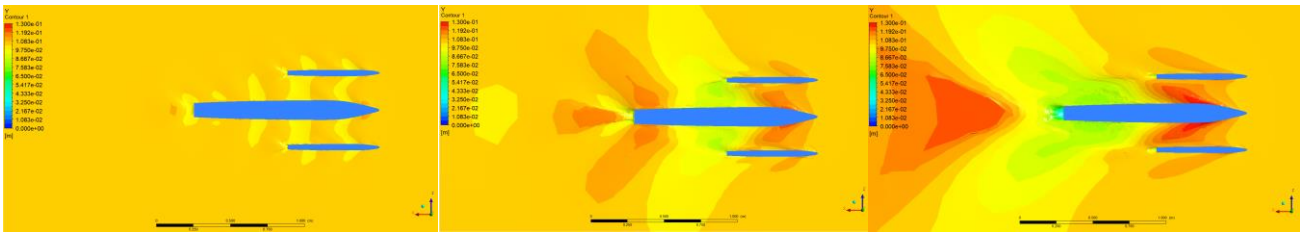

(a) Fr = 0.2 (b) Fr = 0.4 (c) Fr = 0.6

Figure 12. Velocity Distribution of Trimaran C

The presence of fluid interactions between the main hull and side hull in the Trimaran model is seen in Figures 10-12. At low speeds with Fr=0.2, it demonstrates that interference is not very substantial, but in this Trimaran version, it has no effect on the overall resistance coefficient. Furthermore, when Fr=0.4, the interaction of the Trimaran model happens fairly strongly, increasing the resistance of the Trimaran ship. Trimaran C has the largest overall resistance coefficient compared to other trimaran models because the side hull location at the front has a higher influence on wave interaction, as illustrated in Figure 10(c) - 12 (c). This interaction has implications for the forces acting on the main hull and side hull. $C_T$ readings change significantly depending on longitudinal side hull placement. Non-interference Trimaran has a lower $C_T$ than previous variants, with an average difference of 2.8% versus Trimaran A, 4.6% vs Trimaran B, and 6.8% versus Trimaran C. The interference effect between the main hull and side hull trimaran models is responsible for this discrepancy.

A significant increase in resistance occurs in Trimaran C with R/L=0.5 with a side hull parallel to the main hull for the bow section where the fluid flow impacts all three bow sections of the hull simultaneously. This generates a sequence of waves to converge due to the combinations of the side hull and the main hull. The consequence of this incident is the increase of a substantial escalation in wave interference in the region surrounding the bow of the trimaran model, as shown in Figure 12 (c). This is also confirmed by the results of the calculation of the interference between the trimaran hulls shown in Figure 13, where the increase in the value of the Trimaran C interference factor is more significant than the increases within rates of the other Trimaran variations. A significant increase in the total resistance coefficient occurred at Fr > 0.4, this was caused by the dominant interaction between trimaran hulls. trimaran hull interactions consist of wave interactions due to hull form and viscous interactions as mentioned in Jamaluddin et al. [21].

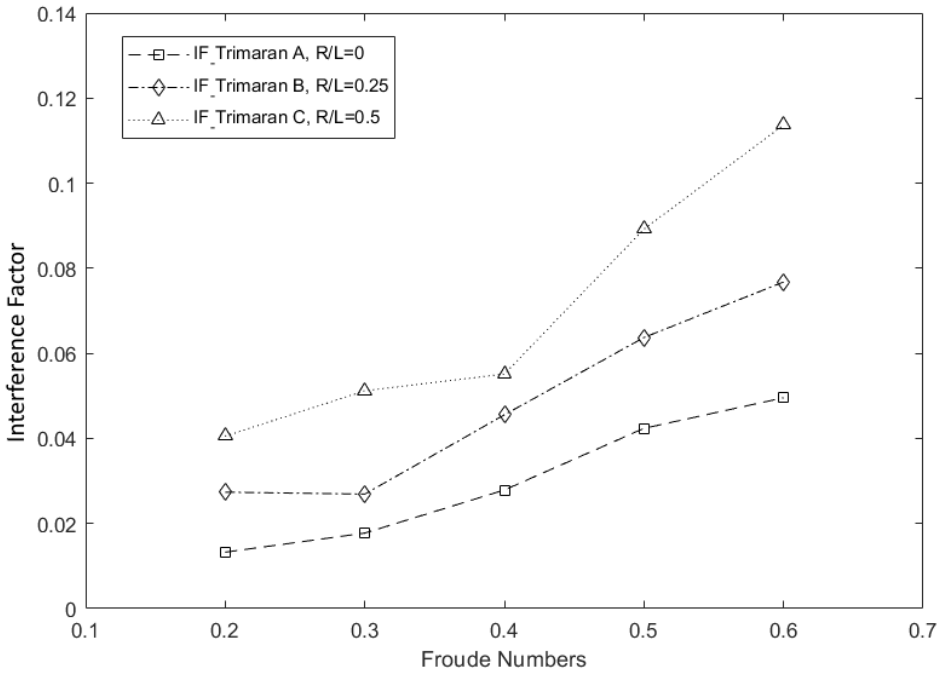


Figure 13. Interference Factor of Trimaran

The phenomenon that appears is an increase in the elevation of the waves between the main hull and the side hull of the trimaran. Due to the interaction between the waves generated by the main hull and those generated by the side hull, this superposition phenomenon occurs. The increase in resistance occurs in proportion to the increase in interference between the hulls on the trimaran. As shown in Figure 13, interference on Trimaran C occurs significantly. Then on trimaran B occurs lower and Trimaran A shows the smallest interference phenomenon. However, it is necessary to conduct further investigations to determine the interference component of the resistance that occurs between hulls in these trimaran models.

## 4. Conclusion

This research demonstrates that CFD makes a great contribution to the estimation of resistance on trimaran ships with and without interference at S/L=0.2.Trimaran performs CFD simulations with three different side hull positioning modifications along the longitudinal axis (R/L). The outcomes of this simulation demonstrate that the Wetted Surface Area and form factor of the model make a significant contribution to resistance. Apart from it, longitudinal side hull placement on trimaran ships affects drag, where Trimaran A has low resistance, with an average of 1.7% lower than Trimaran B and 3.9% than Trimaran C.

The difference in resistance is caused by the longitudinal positioning of the side hull, which affects the amount of interference between the trimaran hulls, increasing average resistance of 2.8% against Trimaran A, 4.6% against Trimaran B, and 6.8% against Trimaran C. The simulation results show that the Trimaran C has the greatest $C_T$ value than other variations this is due to interference between trimaran hulls which has a quite significant impact due to an increase in wave intersection around the bow of the trimaran model.

## Acknowledgments

The authors thank the University of Pattimura for funding the research project under contract no. 1999/UN13/SK/2020.

## References

[1] M. Ramdhan and A. Taslim, "Aplikasi Sistem Informasi Geografis Dalam Penilaian Proporsi Luas Laut Indonesia," *Jurnal Ilmu Geomatika*, vol. 19, no. 6, pp. 141–146, 2013.

[2] M. H. Yudhistira and Y. Sofiyandi, "Seaport status, port access, and regional economic development in Indonesia," Maritime Economics & Logistics, vol. 20, no. 4, pp. 549–568, Dec. 2018, doi: 10.1057/s41278-017-0089-1.

[3] Z. Elcin, "Wave Making Resistance Characteristics of Trimaran Hulls," Naval Postgraduate School, Canada, 2003.

[4] R. B. Luhulima, I. K. A. P. Utama, and A. Sulisetyono, "Experimental Investigation into the Resistance Components of Displacement Trimaran at Various Lateral Spacings," *International Journal Engineering Research Science*, vol. 2, no. 7, pp. 2395-6992, 2016.

[5] B. Yildiz, B. Sener, S. Duman, and R. Datla, "A numerical and experimental study on the outrigger positioning of a trimaran hull in terms of resistance," *Ocean Engineering.*, 2020, doi: 10.1016/j.oceaneng.2020.106938.

[6] Y. Chen, L. Yang, Y. Xie, and S. Yu, "The Research on Characteristic Parameters and Resistance Chart of Operation and Maintenance Trimaran in the Sea," *Polish Maritime Research*, 2016, doi: 10.1515/pomr-2016-0041.

[7] Alexander W. Gray, "A Preliminary Study of Trimarans," *West Virginia Univ.*, 2003.

[8] M. Heidari *et al.*, "Numerical analysis of side hull configuration in Trimaran," *Rev. Int. Métodos Numéricos para Cálculo y Diseño en Ing.*, vol. 35, no. 2, pp. 1–17, Jun. 2019, doi: 10.23967/j.rimni.2019.06.004.

[9] Sutiyo and I. K. A. P. Utama, "CFD Analysis into the Drag Characteristics of Trimaran Vessel: Comparative Study between Standard NPL 4a and the use of Axe-Bow," IOP Conference Series: Earth and Environmental Science, vol. 799, no. 1, p. 12007, Jun. 2021, doi: 10.1088/1755-1315/799/1/012007.

[10] C. H. Son, "CFD Investigation of Resistance of High-Speed Trimaran Hull Forms," Florida Institute of Technology Melbourne, Florida, 2015..

[11] G. A. P. Poundra, I. K. A. P. Utama, D. Hardianto, and B. Suwasono, "Optimizing trimaran yacht hull configuration based on resistance and seakeeping criteria," in *Procedia Engineering*, 2017, doi: 10.1016/j.proeng.2017.08.124.

[12] C. Sun, C. Guo, C. Wang, L. Wang, and J. Lin, "Numerical and Experimental Study of Flow Field between the Main Hull and Demi-Hull of a Trimaran," *Journal of Marine Science and Engineering*, vol. 8, no. 12, p. 975, 2020, doi: 10.3390/jmse8120975.

[13] I. K. A. P. Utama, Sutiyo, and I. K. Suastika, "Experimental and Numerical Investigation into the Effect of the Axe-Bow on the Drag Reduction of a Trimaran Configuration," *International Journal of Technology*, vol. 12, no. 3, pp. 527–538, Jul. 2021, doi: 10.14716/ijtech.v12i3.4659.

[14] J. H. Ferziger and M. Perić, *Computational Methods for Fluid Dynamics*. Berlin, Heidelberg: Springer Berlin Heidelberg, 2002.

[15] J. D. Anderson, *Computational Fluid Dynamics: The Basics with Applications*. New York, USA. pp. 526-532: McGraw-Hill, 1995.

[16] F. R. Menter, "Two-equation eddy-viscosity turbulence models for engineering applications," *AIAA J.*, vol. 32, no. 8, pp. 1598–1605, Aug. 1994, doi: 10.2514/3.12149.

[17] F. R. Menter, M. Kuntz, and R. Langtry, "Ten Years of Industrial Experience with the SST Turbulence Model," in *4th Internal Symposium, Turbulence, heat and mass transfer*, 2003, pp. 625–632.

[18] A. G. Elkafas, M. M. Elgohary, and A. E. Zeid, "Numerical study on the hydrodynamic drag force of a container ship model," *Alexandria Engineering Journal*, vol. 58, no. 3, pp. 849–859, Sep. 2019, doi: 10.1016/j.aej.2019.07.004.

[19] C. L. Ford and P. M. Winroth, "On the scaling and topology of confined bluff-body flows," *Journal of Fluid Mechanics*, 2019, doi: 10.1017/jfm.2019.583.

[20] ANSYS, *ANSYS CFX-Solver Theory Guide*. Canonsburg, PA, USA: Ansys Inc, 2020.

[21] A. Jamaluddin, I. K. A. P. Utama, B. Widodo, and A. F. Molland, "Experimental and numerical study of the resistance component interactions of catamarans,"Proceedings of the Institution of Mechanical Engineers, Part M: Journal of Engineering for the Maritime Environment., vol. 227, no. 1, pp. 51–60, Feb. 2013, doi: 10.1177/1475090212451694.